# Use of a bioelectronic tongue for the monitoring of the photodegradation of phenolic compounds

*Xavier Cetó,*[a,b] *Andreu González-Calabuig,*[a] *Manel del Valle*[a]*

[a] Sensors and Biosensors Group, Department of Chemistry, Universitat Autònoma de Barcelona, Edifici Cn, 08193 Bellaterra, Barcelona, Spain
[b] Mawson Institute, University of South Australia, Mawson Lakes, South Australia 5001, Australia
* e-mail: manel.delvalle@uab.cat

Received:
Accepted:

**Abstract**

The application of a voltammetric bioelectronic tongue for the simultaneous monitoring of catechol, *m*-cresol and guaiacol in wastewater is reported. Voltammetric responses obtained from an array of bulk modified (bio)sensors, containing enzymes such as tyrosinase and laccase, were combined with chemometric tools such as artificial neural networks (ANNs) for building the quantitative prediction model. To this end, the chemometric model was first built employing a factorial design, validated employing an external test set of samples (n=14; total NRMSE of 0.076), and afterwards applied to the monitoring of the mineralization of the three phenol pollutants during a photo-Fenton advanced oxidation process.

**Keywords:** Electronic Tongue; Artificial Neural Network; voltammetric biosensor; phenolic compounds; wastewater

DOI: 10.1002/elan.

## 1. Introduction

Phenolic compounds are widely used in industry as chemical antioxidants, chemical intermediates, additives to lubricants and gasoline, disinfectants, tanning agents, photographic developers or in the production of drugs and pesticides, among others [1-3]. However, despite its extensive usage, some of them are avowed to possess adverse health effects and are consequently regulated, for example by the US Environmental Protection Agency (EPA) or the European Union (EU), as priority pollutants due to their toxicity and persistence in the environment [4, 5].

Beside industrial sources, large quantities of phenol-polluted waters are also formed from e.g. the production of olive oil (olive oil mill wastewater, OMW) in the main olive producing countries in the Mediterranean region [6]. The phenolic compounds present on those are considered major contributors to the toxicity and the antibacterial activity of OMW, and limit their microbial degradability [7].

For these reasons, removal and control of phenolic compounds from wastewaters is a critical issue, affecting many different industrial sources. On that account, several methods have been reported in the literature to tackle elimination of organic pollutants in water [3, 8-11]; e.g. incineration, air stripping, air desorption, liquid-liquid extraction, adsorption of the organic compounds onto activated carbon, inverse osmosis, ultra-filtration, biological treatment, wet oxidation, electrochemical oxidation, photochemical oxidation or chemical oxidation, etc. Even, in some cases, the elimination of organic pollutants needs the coupling of two or more of those basic treatment techniques [9, 12].

Among the different alternatives, advanced oxidation processes (AOPs) have been reported as very promising methods for the treatment of hardly biodegradable organic pollutants [13, 14]. AOPs are based on the generation of highly reactive radicals (especially hydroxyl radicals) in near ambient temperature and pressure conditions, which are extraordinarily reactive species that attack most of the organic molecules. The most common AOPs are UV-based and $H_2O_2$-based processes like the heterogeneous photocatalysis with UV/$TiO_2$, or the Fenton and photo-Fenton reactions [13, 14].

Concerning the detection of phenolic compounds [15], the official analytical methods are based on liquid-liquid extraction for liquid samples, and Soxhlet extraction for solid samples, followed by gas chromatography using different detection devices, normally requiring a derivatization step [2]. Unfortunately, these methods take long time, and require expensive and hazardous organic solvents, which are undesirable for health and disposal reasons. Hence, there is a general trend to change these procedures to solid phase extraction (SPE) and liquid chromatography, or capillary electrophoresis methods to avoid some of these inconvenients [15]; still, these require the use of heavy laboratory equipment, long time analysis and are unsuitable for on-site analyses.

In this direction, biosensors provide an alternative solution for the determination of phenolic compounds thanks to their low cost, fast response and because they can be easily used to carry out on-field analyses [16]. Even more, the usage of chemometric tools such as artificial neural networks (ANNs) might help to avoid and/or take into account any interference problem derived from additional species [17]; the coupling of the two concepts leads to an approach known as (bio)electronic tongue (BioET) [18]. That is, a new class of ETs characterized by the incorporation of one or several biosensors into the sensor array, which might be combined with common chemosensors [19]. Thus, with this methodology, it is possible to achieve a parallel determination of a large number of different species, while any interference effect is solved using these advanced chemometric tools [20].

Based on the foregoing, the aim of this work is to demonstrate the applicability of a voltammetric system employing the electronic tongue principles for the monitoring of different phenolic pollutants in wastewaters. The proposed approach is based on the coupling of cyclic voltammetric responses obtained from an array of enzymatic voltammetric (bio)sensors, with chemometric tools such as ANNs for building the quantitative prediction models. To this aim, catechol, *m*-cresol and guaiacol mixtures were selected as the study case, as they are common phenolic compounds present in various industrial effluents but of difficult removal by conventional wastewater treatment schemes [21]. Firstly, an ANN response model to predict the three concentrations was built and validated, while, at a second stage, a monitoring application during the mineralization of a mixture with the three compounds was performed.

## 2. Experimental

### 2.1. Reagents and solutions

All reagents used were analytical reagent grade; all solutions were prepared using deionised water from a Milli-Q system (Millipore, Billerica, MA, USA). Tyrosinase from mushroom (EC 1.14.18.1, 4276 $U \cdot mg^{-1}$), laccase from *Trametes versicolor* (EC 1.10.3.2, 21 $U \cdot mg^{-1}$), copper nanoparticles (<50 nm), catechol, *m*-cresol, guaiacol, potassium dihydrogen-phosphate, potassium monohydrogenphosphate and hydrogen peroxide 30% (w/w) were purchased from Sigma-Aldrich (St. Louis, MO, USA). Ammonium sulphate was purchased from JT Baker (Deventer, Netherlands). Magnesium sulphate heptahydrate, manganese (II) sulphate monohydrate and iron (II) sulphate heptahydrate were purchased from Panreac Química (Barcelona, Spain). Potassium chloride was obtained from Merck KGaA (Darmstadt, Germany). Graphite powder (particle size 50 μm) was used as received (BDH Laboratory Supplies, Poole, UK). Epotek H77 resin and its corresponding hardener were supplied from Epoxy Technology (Billerica, MA, USA). Compact UV bulb lights (254nm wavelength peak, 25W) were purchased from a local distributor (Eventlights, Barcelona, Spain).

Buffered Artificial wastewater (AWW) was prepared by mixing 0.50g of $(NH_4)_2SO_4$, 1.00g of $MgSO_4 \cdot 7H_2O$, 0.10g of $MnSO_4 \cdot H_2O$, 0.005g of $FeSO_4 \cdot 7H_2O$ per liter of tap water [22].

### 2.2. Building the response model - experimental design

Before using the BioET as a tool for the monitoring of the photodegradation process, the quantitative response model to predict the phenolics mixture composition from the cyclic voltammograms had first to be built. The objective of this step is to determine an ANN configuration that has best prediction abilities of the phenolics mixture composition. Additionally, the performance of the built model has to be validated towards new samples; that is, to ensure its accuracy and precision with unbiased data.

To build the response model, a $3^3$ factorial design was used to define the set of samples for the training subset (27 samples) [23, 24]; while the set of samples used for the testing subset (14 samples) were randomly distributed along the experimental domain (with concentrations from 0 to 80 $mg \cdot L^{-1}$ for each phenolic compound). Besides, as the response of the enzymatic sensors is pH-sensitive, all the samples were prepared

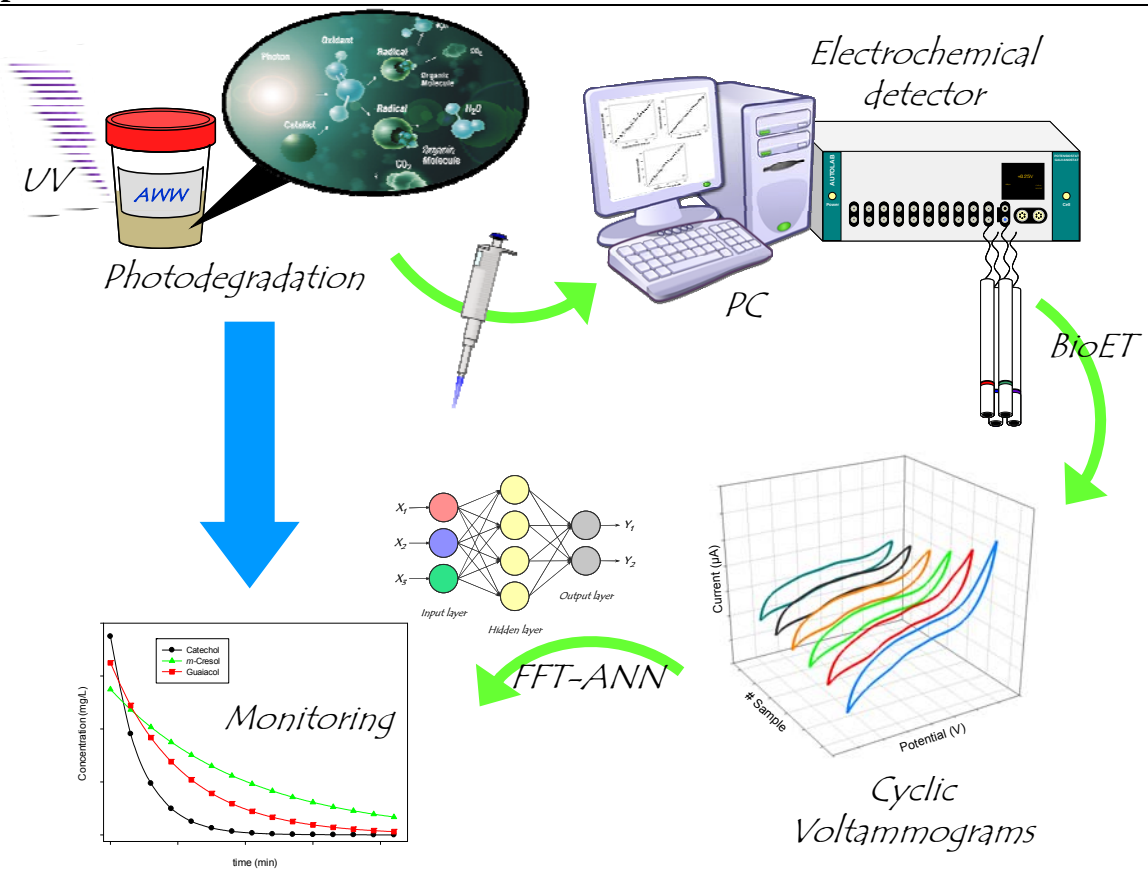


Fig. 1. Scheme of the experimental setup used for the photodegradation and monitoring of the phenolic compounds.

in buffered media (0.1 M phosphate buffer at pH 6.50 and 0.1 M KCl saline background).

### 2.3. Photodegradation process

Several methods are reported in the literature to tackle the elimination of organic pollutants in aqueous solutions [9, 11, 13, 25]. However, as the aim of the present work was to demonstrate the capabilities of BioETs as a tool for the monitoring of water contaminants, rather than focusing on the methods used for its removal, the photo-Fenton process was chosen as the treatment method due to its simplicity and efficiency [9, 12].

Experimental conditions were adapted from previous works [9, 26]; and a representation of the experimental set-up used is sketched in Figure 1. Briefly, a mixture of the phenolic compounds under study was prepared in AWW as the medium, in order to better simulate a real monitoring application. The oxidation process was performed in a stirred batch photo reactor equipped with two 25 W UV lights, and protected from the incidence of direct sunlight. The use of a thermostated bath was discarded as any appreciable increase of the temperature was not noticed, in part thanks to the short reaction time; therefore, reaction took place at room temperature (25±3ºC). The beginning of the experiment corresponded to the simultaneous addition of hydrogen peroxide and the start of irradiation.

In a typical run, 1 L of a AWW solution containing the ternary mixture of phenolic compounds was mixed with 36 mg of $FeSO_4 \cdot 7H_2O$ and 1440 μL of $H_2O_2$ 30%.

For the monitoring of the photodegradation process with the BioET, a 9 mL aliquot of the reaction mixture was taken from the reactor at specific times with a micropipette, and diluted 1:1 with buffer solution (0.1 M phosphate buffer + 0.1 M KCl at pH 6.50) to avoid any discrepancies in the biosensors response due to variation of the pH. This was preferred rather than adjusting the pH of the AWW or the aliquot as this would simplify its future operation; that is, avoiding the need to perform any other sample step or pre-treatment rather than its mere dilution. Then, the diluted sample was measured with the voltammetric BioET. In this way, *at-line* monitoring was achieved with a delay in the measurements of ca. 15-20s.

Lastly, after sample measurement, voltammetric

responses were input to the ANN model through its preprocessing with Fourier transform for feature extraction/data compression, and final concentration of each compound was obtained by multiplying the resulting values by the proper dilution factor.

### 2.4. Electronic tongue approach

The voltammetric BioET was formed by an array of 4 (bio)sensors, plus a reference double junction Ag/AgCl electrode (Thermo Orion 900200, Beverly, MA, USA) and a commercial Pt counter electrode (Model 52-67, Crison Instruments, Barcelona, Spain).

Working electrodes were bulk-modified graphite-epoxy composites, which were prepared by mixing the resin, graphite powder and the modifier/enzyme in the ratio 83:15:2 (w/w), or 82:15:2:1.5 in the case of the bienzymatic biosensor (laccase and tyrosinase, respectively) [27, 28]. Afterwards, resin was allowed to harden at 40 ºC for seven days, and electrode surfaces were polished with different sandpapers of decreasing grain size; with a final geometric area of 28 $mm^2$.

In this manner, the array of 4 voltammetric electrodes was prepared, consisting in one blank electrode plus three (bio)composite electrodes modified with tyrosinase, tyrosinase+laccase and Cu nanoparticles. This choice was intended as to maximize the response of the (bio)sensor array towards phenolic compounds. That is, on one side, tyrosinase and laccase were chosen as they are extensively used for the development of amperometric biosensors aimed to the detection of phenolic compounds [29]. Whereas, on the other side, copper nanoparticles were also considered as the two enzymes are copper-containing proteins; hence, due to the well-known catalytic properties of nanoparticles and the importance of copper in the enzymes catalytic center, its inclusion was considered of potential interest.

Electrochemical measurements were performed at room temperature (25ºC), using a 6-channel AUTOLAB PGSTAT20 (Ecochemie, Netherlands) controlled with GPES Multichannel 4.7 software package. A complete voltammogram was recorded for each sample by cycling the potential between -0.4 V and +0.8 V vs. Ag/AgCl with a step potential of 9 mV and a scan rate of 100 $mV \cdot s^{-1}$.

In order to get stable voltammetric responses, and to ensure reproducible signals from the BioET array along the whole experiment, two extra precautions were taken. Firstly, electrodes were cycled in buffer solution after its polishing and beginning of sample measurements. Secondly, an electrochemical cleaning stage was carried out between measurements to prevent any fouling or accumulation of impurities on the working electrode surfaces. To this end, a conditioning potential of +1.0 V was applied during 40 s in a cell containing 20 ml of distilled water [30].

### 2.5. Data processing

Chemometric processing of the data was done in MATLAB 7.1 (MathWorks, Natick, MA, USA) using specific routines written by the authors, and its Neural Network Toolbox (v.4.0.6); while representation and analysis of the results was performed using Sigmaplot (Systat Software Inc., San Jose, CA, USA).

To fully exploit all the information obtained from each voltammogram and to prevent the under-determination problem encountered with an oversized ANN with excessively complex data (i.e. when too few data points are available compared with the number of adjustable parameters) [31], a compression step was performed to decrease the dimensionality of the electrochemical signatures. The main objective of this step is to reduce the complexity of the input signal preserving the relevant information, which in addition allows to gain advantages in training time, to avoid redundancy in input data and to obtain a model with better generalization ability [31, 32].

In our case, compression of voltammetric data was achieved by means of fast Fourier transform (FFT) [27], while ANNs were chosen as the modelling tool to achieve the individual quantification of each of the compounds. In this manner, each voltammogram was compressed down to 32 coefficients without significant loss of information (details provided in Supporting information), and obtained coefficients were then used as inputs to the ANN model.

Moreover, to contrast the performance of FFT as preprocessing tool, discrete Wavelet transform (DWT) was also used for data compression (with Daubechies mother wavelet) and its results were used as reference to compare with the ones obtained with FFT [33]. Details from the compression to the model optimization and performance, for both strategies, can be found in Supporting information.

## 3. Results and Discussion

### 3.1. BioET array response

As already stated, prior to using the BioET as a

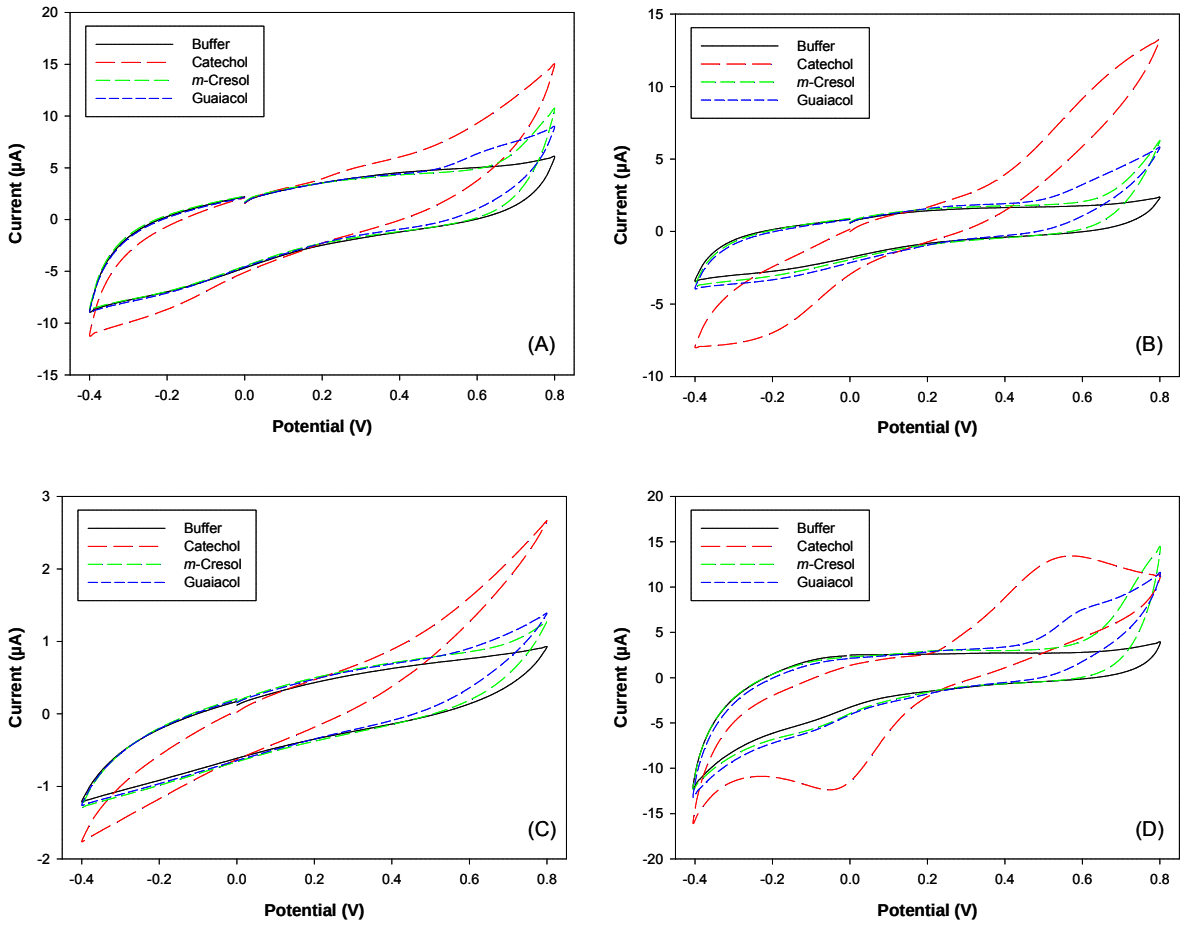


Fig. 2. Example of the different voltammograms obtained with (A) graphite–epoxy sensor, (B) tyrosinase modified biosensor, (C) tyrosinase+laccase modified biosensor and (D) Cu nanoparticle modified electrode for buffer and stock solutions of each of the three phenolic compounds considered (23 mg·L$^{-1}$).

monitoring tool of the phenolic compounds photodegradation process, a response model was built. To this aim, a total set of 41 phenolics trinary mixtures, with concentration range from 0 to 80 mg·L$^{-1}$ for each compound was first analyzed and used to build and validate the ANN model; so that afterwards, it may be used for the simultaneous monitoring of mineralization of the compounds under scrutiny.

In first instance, voltammetric responses for each of the electrodes towards individual compounds should also be checked. That is, to ensure that enough differentiated signals were observed for the different electrodes, generating rich data that might be a useful departure point for the multivariate calibration model.

To this aim, under the described conditions in section 2.4, individual stock solutions of catechol, *m*-cresol and guaiacol were analyzed and their voltammograms inspected (Figure 2). Basically, two processes could be observed there: the oxidation of the corresponding phenol to its quinone form, and the reduction of the quinone to the phenolic form, as previously reported [29]. Besides, clearly differentiated curves are obtained for each of the considered compounds and for each electrode, the desirable condition for an ET study.

In addition, the benefits derived from the incorporation of the enzymatic biosensors may also be noticed, for which higher currents were obtained, especially in the reduction region close to 0 V where obtained net current is clearly enlarged; a situation more patent for catechol and *m*-cresol, which do not show any response with the bare electrode in that region. Similarly, some catalytic effect can also be observed for the sensor modified with copper nanoparticles, a fact somehow explained given both tyrosinase and laccase are copper-containing redox enzymes.

Therefore, once it was confirmed that differentiated behaviour was observed by the BioET array towards the different compounds under study, the next step was to proceed with the building of the ANN model.

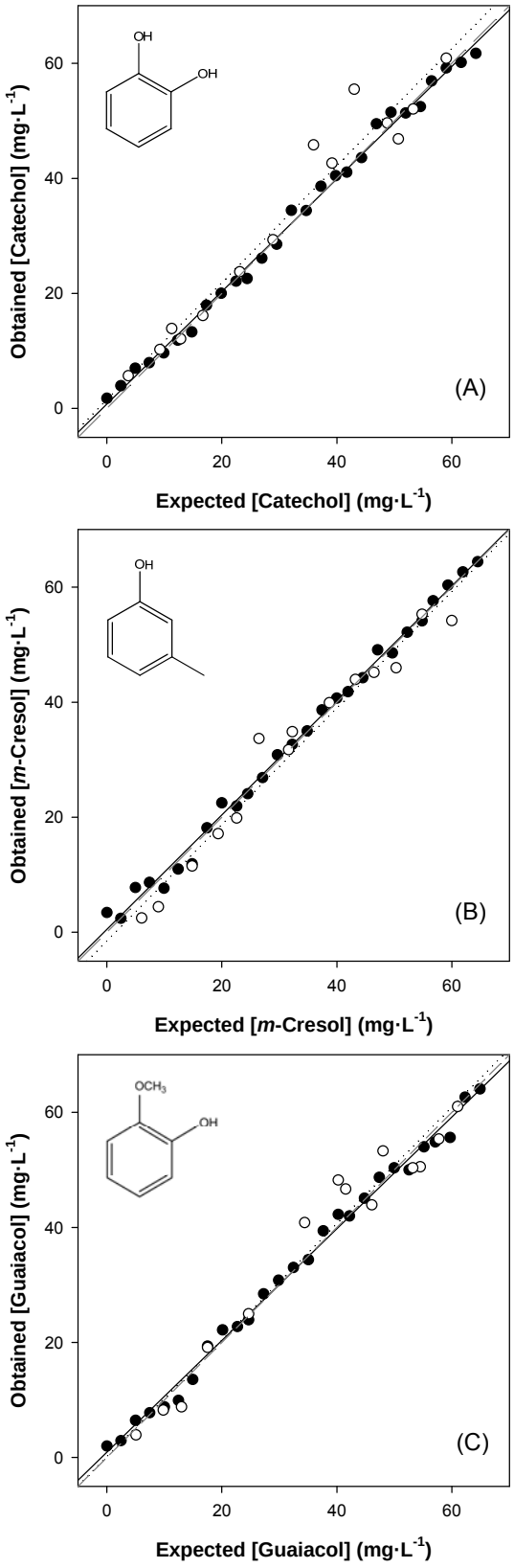


Fig. 3. Modelling ability of the optimized FFT-ANN. Comparison graphs of obtained vs. expected concentrations for (A) catechol, (B) *m-cres*ol and (C) guaiacol, both for training (●, solid line) and testing subsets (○, dotted line). Dashed line corresponds to theoretical *Y*=*X* diagonal line.

### 3.2. Building of the ANN model

Under the conditions previously described, the training and testing sets of samples were measured employing the multielectrode array, obtaining a complete voltammogram for each of the (bio)sensors, and each sample.

However, the large dimensionality of the data generated when voltammetric sensors are used (i.e. samples x sensors x polarization potentials) hinders their treatment; especially if ANNs are to be used. Therefore, raw voltammetric responses were compressed down to 32 coeffs. by means of FFT, which allowed for a compression of the original information up to 88.1% (details provided in Supporting information). Besides the high compression ratio, FFT is also particularly useful because of its ability to compress data and to remove noise (high frequency changes in signal) at the same time [32].

The next step was the building and optimization of the ANN model, which is a trial-and-error process where several parameters (e.g. training algorithm, number of hidden layers, number of neurons, transfer functions, etc.) are fine-tuned in order to find the best configuration that optimizes the performance of the model. For this, the ANN model was first trained employing data from the training subset, and its performance evaluated employing the samples from the testing subset; this allowed to characterize the accuracy of the quantification model and to detect any overfitting situation due to the use of unbiased data.

After a systematic evaluation of different topologies, from a total number of 90 different configurations (details provided in Supporting information), the final architecture of the ANN model had 128 neurons (4 sensors × 32 FFT coeffs.) in the input layer, 5 neurons and *logsig* transfer function in the hidden layer and 3 neurons and *tansig* transfer function in the output layer, providing simultaneously the concentration of the three phenolic compounds considered.

Subsequently, comparison graphs of predicted vs. expected concentrations, both for training and testing subsets, for each of the compounds were then built to check the prediction ability of the obtained ANN model (Figure 3). It may be seen that a satisfactory trend is obtained, with regression lines almost indistinguishable from the theoretical one (slope = 1, intercept = 0), this condition especially significant for the external test set.

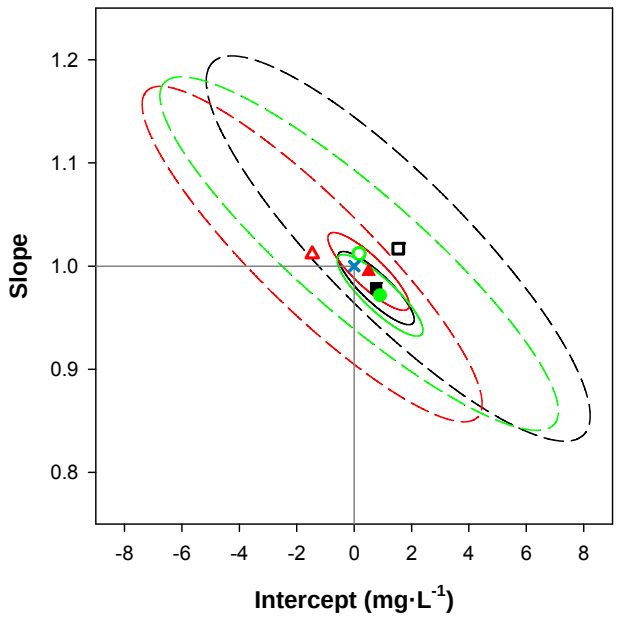


Fig. 4. Joint confidence intervals for the three species: (●) catechol, (▲) *m-cre*sol and (■) guaiacol, both for training (filled symbols, solid lines) and testing (empty symbols, dashed lines) subsets. Also ideal point (1,0) is plotted (x); intervals calculated at the 95% confidence level.

Table 1. Results of the fitted regression lines for the comparison between obtained vs. expected values, both for the training and testing subsets of samples and the three considered species (intervals calculated at the 95% confidence level).

| ***Training subset*** | | | | | |
|---|---|---|---|---|---|
| *Compound* | *r* | *Slope* | *Intercept* | *RMSE* | *Total RMSE* |
| Catechol | 0.998 | 0.979±0.028 | 0.76±1.05 | 0.025 | |
| *m*-Cresol | 0.997 | 0.995±0.030 | 0.50±1.12 | 0.029 | 1.50 |
| Guaiacol | 0.997 | 0.972±0.031 | 0.90±1.19 | 0.023 | |
| ***Testing subset*** | | | | | |
| *Compound* | *r* | *Slope* | *Intercept* | *RMSE* | *Total RMSE* |
| Catechol | 0.975 | 1.017±0.146 | 1.54±5.23 | 4.80 | |
| *m*-Cresol | 0.981 | 1.012±0.127 | -1.46±4.63 | 3.63 | 4.20 |
| Guaiacol | 0.979 | 1.012±0.134 | 0.17±5.43 | 4.09 | |

RMSE: Root Mean Square Error; Intercept and RMSE values are expressed in mg·L$^{-1}$

### 3.3. Accuracy and precision of the ANN model

After optimization and selection of the ANN architecture, next step was to evaluate its performance and accuracy employing the data from the tesing subset. That is, to determine whether or not the concentrations estimated by the ANN model statistically differ from the nominal concentrations, when presenting new samples to it. To this aim, regression statistics were evaluated in two different manners, using *t* and F distribution based tests [34].

Firstly, regression parameters of the comparison graphs were calculated (Table 1), and as deduced from the graphs, a satisfactory linear trend is observed for all the cases, with regression lines almost indistinguishable from the theoretical ones. But, as usual in data modelling, with an improved behaviour for the training subset due to the lower dispersion attained. However, since the external testing subset data is not employed at all for the modelling, its goodness of fit is a more correct indicator of the accomplished modelling performance. Nevertheless, the results obtained for both subsets are close to the ideal comparison values (slope 1, intercept 0 and correlation coefficient 1), being these values included in the confidence intervals.

Additionally, joint confidence intervals were calculated and plotted according to advanced linear regression methodology [34]. The usage of this plot constitutes a rapid visualization tool to detect if there are or not differences between two compared methods, judging simultaneously the goodness of slope and intercept. Thus, taking into account the uncertainties in both axes to calculate the estimated covariance matrix based on an F distribution. Hence, we examined whether the theoretical comparison point (1,0) was included in the elliptical region of the joint confidence intervals of slope and intercept for plots shown in Figure 3. As can be observed in Figure 4, the point (1,0) is included in the confidence intervals for the three species, both for the training and testing subsets; thus confirming that statistically, there are no significant differences for the BioET predicted values and the real ones. Again, it can be seen how results obtained for the training subset are more precise, but with remarkable satisfactory accuracy for both subsets; being all of them close to the ideal point (1,0). The fact that bigger confidence intervals are obtained for the external test subset can be explained by two simple facts. On one side, this data is not employed at all during the building of the model, then being a true test of its generalization ability. On the other side, the number of samples in the testing subset is lower, and consequently, the tabulated values of *t* and F are higher, which implies higher confidence intervals.

Lastly, as an additional verification of the proposed approach, a Student's paired samples *t* test for the external test subset was performed. Obtained experimental *t* values were 1.73, 1.13 and 0.54 for catechol, *m*-cresol and guaiacol respectively, while the critical tabulated *t* value with 95% confidence level

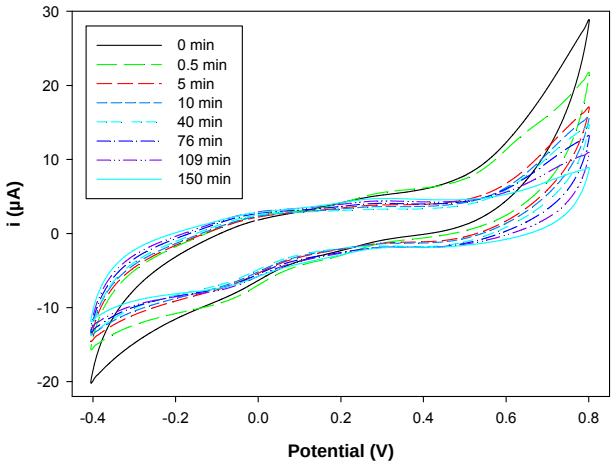


Fig. 5. Voltammetric responses obtained for some samples collected during the photodegradation process with the Cu nanoparticle modified sensor, as example.

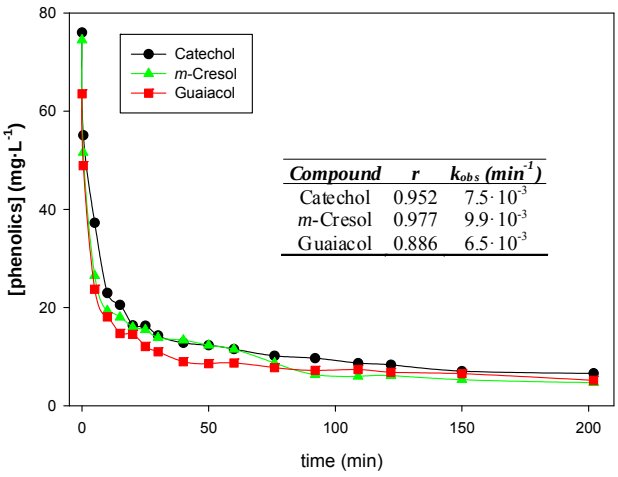


| *Compound* | *r* | $k_{obs}$ ($min^{-1}$) |
|---|---|---|
| Catechol | 0.952 | $7.5 \cdot 10^{-3}$ |
| *m*-Cresol | 0.977 | $9.9 \cdot 10^{-3}$ |
| Guaiacol | 0.886 | $6.5 \cdot 10^{-3}$ |

Fig. 6. Photo-Fenton mineralization and its monitoring with the BioET. Representation of the found values for each of the considered species: (●) catechol, (▲) *m-cres*ol and (■) guaiacol. Inset table corresponds to the calculated apparent pseudo-first-order rate constants ($k_{obs}$), determined from the linealizations.

and 13 degrees of freedom is 2.16. Therefore, from the comparison graphs and these t test results, it could be again concluded that there are no significant differences between the ET predicted values and the real ones.

### 3.4. Monitoring of phenolics mineralization

After building and validating the generated model, the next step was the application of the proposed ET towards the monitoring of the photodegradation process of phenolic compounds mixtures.

To this aim, a trinary mixture of catechol, *m*-cresol and guaiacol (72.8 $mg \cdot L^{-1}$, 69.4 $mg \cdot L^{-1}$ and 65.6 $mg \cdot L^{-1}$, respectively) was prepared in AWW. Then, its photodegradation was carried out as described in section 2.3. During the process, aliquots of the solution from the photoreactor were removed at specific times from the beginning to up to ca. 200 min, and measured with the BioET with no further pretreatment than its mere dilution 1:1 with buffer solution. Recorded voltammetric responses were then preprocessed with FFT, and obtained coefficients were input into the previously built model which allowed the simultaneous determination of the three compounds. Lastly, actual concentration of each compound in the reactor batch was obtained by multiplying by the proper dilution factor.

An extract of the recorded signals obtained during the photodegradation process is shown in Figure 5, where it can be clearly seen how currents decreased monotonously as reaction progressed. Thus, even from the raw voltammetric responses, it would be possible to monitor the mineralization process (and detect its end point). However, in that case, not allowing the resolution of the different phenolic compounds.

Besides, the use of the BioET might not be limited to monitor the mineralization process, but also to detect whether or not some residual wastewater must be treated. Thus, requiring in that case the quantification of each of the compounds, to determine if their levels are under the required ones; what will be achieved thanks to the use of the chemometric model.

Evolution along time of the photo-Fenton mineralization process is plotted in Figure 6. At first sight, it can be seen how the ANN model confirms what was already expected from the voltammetric responses; that is, an exponential decrease in the concentration of each of the compounds. Moreover, the trends observed agree with previous reported results [9], where degradation rate is described by a first-order kinetics with respect to phenols concentration.

In this direction, and considering an independent behaviour of each phenolic compound (i.e. the compounds not interacting with the others during the degradation) [35], degradation rate for each compound can be described by a pseudo-first order kinetics with respect to its concentration according to eq. (1), where $k_{obs}$ corresponds to the apparent pseudo-first-order rate constant.

$$ln\ C = ln\ C_0 - k_{obs} \cdot t \qquad (1)$$

Thus, the plotting of the *ln* of the concentration of each compound vs. time in every experiment leads to a straight line whose slope is $k_{obs}$. Calculated values are summarized in the inset table in Figure 6, where also the obtained correlation coefficients for the linearized least squares regression are detailed, corroborating the pseudo-first order kinetics. As an extra validation, it has to be said that these results coincide with those reported in the literature, e.g. [9, 12].

Therefore, it has been demonstrated that ETs (i.e. the combination of voltammetric measurments with chemometric tools) are an analytically powerful approach for the speciation of different phenolic compounds in wastewater and the monitoring of its mineralization. This approach is particularly useful since it does not only allow the identification of the presence of the phenolic compounds, but also the individual quantification of the amount present in the mixtures analyzed. Besides, with the same experimental setup, the approach proposed herein might be alternatively applied for the quantification of analogous or different mixtures, even quaternary or more complex mixtures, with a proper retraining set of samples. Lastly, this also represents a viable system with significant promise for on-field measurements given its simplicity, rapidity and portability; therefore, really suitable for screening analysis.

## 4. Conclusions

In this work, the application of an ET-based system for the simultaneous monitoring of various phenolic pollutants in wastewater has been reported. More specifically, the approach presented herein combines an array of voltammetric (bio)sensors to extract the fingerprints of the samples along with an ANN model that allows the resolution of signal overlapping and quantification of the individual species. On that account, the complex responses obtained from the (bio)sensor array were successfully processed employing a multilayer ANN; which has proved to be especially suited for building the response models. Lastly, proposed BioET array was then applied to the monitoring of phenol pollutants mixtures degradation during a photo-Fenton process.

Overall, reported approach herein represents a proof of concept for the versatility of the proposed system and its capabilities as on-field screening tool, demonstrating that ETs can be a viable option to monitor several analytes on-site, with the added advantages of simplicity, the low cost of both the system and the analysis, speed of response, versatility, simple measuring setup, etc. With this approach, a quantitative multidetermination of a number of chemical species is easily attainable with rather simple equipment, shifting the complexity from the sensors to the software side.

## Acknowledgements

Financial support for this work was provided by the *Spanish Ministry of Science and Innovation*, MCINN (Madrid) through project CTQ2010-17099. Manel del Valle thanks the support from *Generalitat de Catalunya* and from the program ICREA Academia. Andreu González-Calabuig thanks *Universitat Autònoma de Barcelona* for the PIF fellowship.

## References

[1] Encyclopaedia of Occupational Health and Safety, in J. M. Stellman, D. Osinsky and P. Markkanen (Eds.), International Labour Office, Geneva, **1998**.
[2] K. Farhod Chasib, *J. Chem. Eng. Data* **2013**, *58*, 1549.
[3] S. Mukherjee, B. Basak, B. Bhunia, A. Dey, B. Mondal, *Rev Environ Sci Biotechnol* **2013**, *12*, 61.
[4] EPA, *Steam electric power generating point source category*, *Vol. 47*, Federal Register, **November 1982**, pp. 52290.
[5] Commission Regulation (EEC) Official Journal L 129, Publication Office of the European Union, **18 May 1976**, pp. 23.
[6] L. Gianfreda, G. Iamarino, R. Scelza, M. A. Rao, *Biocatal. Biotransfor.* **2006**, *24*, 177.
[7] R. Capasso, *Current Topics in Phytochemistry* **1997**, *1*, 145.
[8] G. Busca, S. Berardinelli, C. Resini, L. Arrighi, *J. Hazard. Mater.* **2008**, *160*, 265.
[9] M. Rodríguez in *Fenton and UV-VIS based advanced oxidation processes in wastewater treatment: Degradation, mineralization and biodegradability enhancement*, *PhD Thesis,* Universitat de Barcelona, Barcelona, **2003**.
[10] J. M. Britto, M. d. C. Rangel, *Quím. Nova* **2008**, *31*, 114.
[11] S. J. Kulkarni, J. P. Kaware, *International Journal of Scientific and Research Publications* **2013**, *3*, 1.
[12] S. Esplugas, J. Giménez, S. Contreras, E. Pascual, M. Rodríguez, *Water Res.* **2002**, *36*, 1034.
[13] S. Ahmed, M. G. Rasul, W. N. Martens, R. Brown, M. A. Hashib, *Desalination* **2010**, *261*, 3.
[14] I. Magario, F. S. García Einschlag, E. H. Rueda, J. Zygadlo, M. L. Ferreira, *J. Mol. Catal. A,* **2012**, *352*, 1.
[15] D. Puig, D. Barceló, *TrAC Trends Anal. Chem.* **1996**, *15*, 362.
[16] F. Karim, A. N. M. Fakhruddin, *Rev Environ Sci Biotechnol* **2012**, *11*, 261.
[17] Y. Ni, S. Kokot, *Anal. Chim. Acta* **2008**, *626*, 130.

[18] E. Tønning, S. Sapelnikova, J. Christensen, C. Carlsson, M. Winther-Nielsen, E. Dock, R. Solna, P. Skladal, L. Nørgaard, T. Ruzgas, J. Emnéus, *Biosens. Bioelectron.* **2005**, *21*, 608.
[19] J. Zeravik, A. Hlavacek, K. Lacina, P. Skládal, *Electroanalysis* **2009**, *21*, 2509.
[20] M. del Valle, *Electroanalysis* **2010**, *22*, 1539.
[21] C.-H. Ko, S.-S. Chen, *Bioresource Technol.* **2008**, *99*, 2293.
[22] K. Volkan Özdokur, L. Pelit, H. Ertaş, S. Timur, F. Nil Ertaş, *Talanta* **2012**, *98*, 34.
[23] L. Zhang, Y. Z. Liang, J. H. Jiang, R. Q. Yu, K. T. Fang, *Anal. Chim. Acta* **1998**, *370*, 65.
[24] X. Cetó, F. Céspedes, M. I. Pividori, J. M. Gutiérrez, M. del Valle, *Analyst* **2012**, *137*, 349.
[25] O. K. Dalrymple, D. H. Yeh, M. A. Trotz, *J. Chem. Technol. Biotech.* **2007**, *82*, 121.
[26] M. Rodríguez, N. B. Abderrazik, S. Contreras, E. Chamarro, J. Gimenez, S. Esplugas, *Applied Catal. B: Environmental* **2002**, *37*, 131.
[27] X. Cetó, F. Céspedes, M. del Valle, *Talanta* **2012**, *99*, 544.
[28] M. Elkaoutit, I. Naranjo-Rodriguez, K. R. Temsamani, M. D. La Vega, J. L. H. De Cisneros, *J. Agric. Food Chem.* **2007**, *55*, 8011.
[29] R. Solná, P. Skládal, *Electroanalysis* **2005**, *17*, 2137.
[30] X. Cetó, J. M. Gutiérrez, L. Moreno-Barón, S. Alegret, M. del Valle, *Electroanalysis* **2011**, *23*, 72.
[31] F. Despagne, D. L. Massart, *Analyst* **1998**, *123*, 157R.
[32] X. Cetó, F. Céspedes, M. del Valle, *Microchim Acta* **2013**, *180*, 319.
[33] L. Moreno-Barón, R. Cartas, A. Merkoçi, S. Alegret, M. del Valle, L. Leija, P. R. Hernandez, R. Muñoz, *Sens. Actuator B-Chem.* **2006**, *113*, 487.
[34] D. C. Montgomery, E. A. Peck, G. G. Vining, *Introduction to Linear Regression Analysis*, Wiley, Chichester, **2012**.
[35] A. M. Peiró, J. A. Ayllón, J. Peral, X. Doménech, *Applied Catal. B: Environmental* **2001**, *30*, 359.